

1 **Interactions between microfibrillar cellulose and carboxymethyl cellulose**
2 **in an aqueous suspension**

3 Deepa Agarwal, William MacNaughtan, and Tim J. Foster*

4 Division of Food Sciences, School of Biosciences, University of Nottingham, Sutton
5 Bonington Campus, Loughborough, LE12 5RD, UK.

6 *Corresponding author e-mail: tim.foster@nottingham.ac.uk

7

8 **Abstract**

9 New microstructures with interesting, unique and stable textures, particularly relevant to food
10 systems were created by redispersing Microfibrillar cellulose (MFC). This paper reports the
11 interactions between microfibrillar cellulose and carboxymethyl cellulose (CMC) in
12 redispersed aqueous suspensions, by using rheological measurements on variable ratios of
13 MFC/CMC and correlating these with apparent water mobility as determined by time domain
14 NMR. MFC is a network of cellulose fibrils produced by subjecting pure cellulose pulp to
15 high-pressure mechanical homogenisation. A charged polymer such as CMC reduces the
16 aggregation of microfibrillar/fibre bundles upon drying. Small amplitude oscillatory
17 rheological analysis showed the viscoelastic gel-like behaviour of suspensions which was
18 independent of the CMC content in the MFC suspension. A viscous synergistic effect was
19 observed when CMC was added to MFC before drying, leading to improved redispersibility of
20 the suspension. Novel measurements of NMR relaxation suggested that the aggregated
21 microfibrillar/fibre bundles normally dominate the relaxation times (T_2). The dense
22 microfibrillar network plays an important role in generating stable rheological properties and
23 controlling the mobility of the polymer and hence the apparent mobility of the water in the
24 suspensions.

25 **Highlights**

- 26 • CMC improves redispersibility and reduces aggregation of MFC microfibrils
- 27 • NMR relaxation measurements give an insight into the mechanisms of redispersibility
- 28 • Polymer aggregation dominates the T_2 value and NMR behaviour of suspensions
- 29 • Improved re-dispersion is correlated with higher shear viscosity and increased T_2
- 30 • Unique microstructures relevant to foods have been created

31 **Keywords:** Microfibrillar cellulose; carboxymethyl cellulose; low-field NMR; relaxation time;
32 rheology

33 **1. Introduction**

34 Cellulose is the most abundant natural structural polymer in nature and provides mechanical
35 properties such as strength and stiffness to the plant cell wall of higher plants. Important
36 components of this natural fibre strength and stiffness are the microfibrils within the cellulose
37 structure. The fibrous cell wall is essentially a composite material consisting of a framework
38 of cellulose (micro-) fibrils organised into strands of cellulose which are embedded in a matrix
39 of hemicelluloses and lignin. Cellulose microfibrils in the cell wall are intertwined fibrils with
40 a diameter of approx. 2-20nm and a length of 100-40,000nm depending on the source (Kirk
41 and Othmer, 1967; Kocherbitov, Ulvenland, Kober and Jarring, 2008). These cellulose fibres
42 can be broken down into their structural micro/nano-scale units by various chemical and
43 mechanical processes (Henriksson, Berglund and Lindstrom, 2007). Production and
44 characterisation of microfibrillar cellulose (MFC) from wood fibres have been described by
45 Turbak *et al.* 1983 and Herrick *et al.* 1983, where MFC suspensions were obtained by
46 disintegrating cellulose fibres at high shear. The resultant highly entangled MFC network
47 consists of micro/nano size elements with a gel-like behaviour for water suspensions at 1% or
48 lower concentrations of MFC (Turbak *et al.*, 1983, Herrick *et al.*, 1983, Nakagaito and Yano
49 2004, Nishiyama, 2009). During the last decade, microfibrillar cellulose (MFC) has been
50 produced by using more aggressive, high shear or high energy mechanical treatments such as

51 homogenisers or microfluidisers which led to highly entangled, fibril aggregates and
52 mechanically strong networks (Frone *et al.*, 2011, Lavoine *et al.*, 2012). Depending on the
53 pressure, flow rate, temperature, and the design and diameter of the chambers used in high-
54 pressure homogenisers or microfluidisers, different particle size distributions and microfibrillar
55 networks can be produced (Lavoine *et al.*, 2012). Several publications have shown applications
56 of these highly networked MFC microfibrils for various purposes, such as reinforcement in
57 nanocomposites (Malainine, Mahrouz and Dufresne 2005, Lopez-Rubio *et al.*, 2007, Bruce *et*
58 *al.*, 2005), dispersion stabilization (Oza and Frank 1986, Ougiya *et al.*, 1997, Khopade and Jain
59 1990), media filtration (Burger, Hsiao and Chu 2006), antimicrobial action in films (Andresen
60 *et al.*, 2007) and oxygen barrier production in food and pharmaceuticals (Syverud and Stenius
61 2009). The rheological properties of these MFC suspensions have been widely studied by a
62 number of researchers. In general, the rheological properties of aqueous MFC suspensions
63 isolated from softwood, sugar beet pulp, corn cobs and cotton show gel-like behaviour where
64 the storage modulus (G') is higher than the loss modulus (G'') over a wide concentration range
65 (Pääkkö *et al.*, 2007, Tanjawa *et al.*, 2010, Cordabo *et al.*, 2010, Tatsumi *et al.*, 2002, Tatsumi
66 *et al.*, 2007).

67 Homogenisation modifies the structure of the starting materials by releasing microfibrils into
68 the suspension. Drying the MFC is also known to modify the defibrillated state primarily by
69 increased hydrogen bonding but possibly also other forms of bonding such as van der Waals
70 between the microfibrils, leading to the formation of bundles and agglomerates (Quiévy *et al.*,
71 2010). These fibre bundles and aggregates are difficult to redisperse in water in order to form
72 homogeneous suspensions, a consequence being a reduction in the values of rheological
73 parameters such as G' , G'' and the shear viscosity of the suspension. This process of irreversible
74 or partial irreversible agglomeration of cellulosic fibres and stiffening of the polymer structure
75 during drying is known in the literature as hornification. It is a technical term widely used in
76 the paper-making industry (Smook 1990, Kato *et al.*, 1999, Fernandes *et al.*, 2004). The

77 aggregation or agglomeration occurs to varying extents depending on the drying process. To
78 protect the microfibrils from collapse and agglomeration, a number of hydrocolloids, *e.g.* low
79 and high methoxyl pectin, CMC, and sodium polyacrylate, as well as salts *e.g.* sodium chloride
80 (Lowys, Desbrieres & Rinaudo, 2001; Tandjawa *et al.*, 2012; Missoum, Bras & Belgacem,
81 2012), have been used to stabilise the fibrils. Lowys (2001) demonstrated an interaction
82 between MFC and polymeric additives such as sodium-CMC and pectins, where the additives
83 were homogeneously distributed and formed weak bonds with MFC fibres improving the
84 redispersibility of MFC in water. This interaction between the additive and MFC tends to
85 stabilise the fibrils against collapse or agglomeration during the drying process. The objective
86 of the current publication is to provide an insight into the impact of drying (hornification) on
87 the state of the polymer and the apparent water mobility in the MFC matrix.

88 Rheological properties of aqueous suspensions of MFC with or without additives show
89 viscoelastic gel-like behaviour and high viscosity (Cordabo *et al.*, 2010, Agoda-Tandjawa *et*
90 *al.*, 2010). Such properties of aqueous suspensions at 1% (w/w) and lower concentrations, make
91 MFC valuable in a wide range of industrial applications such as food, cosmetics, paints and
92 composites, *etc.* The strong interactions between the MFC fibres in aqueous media are the
93 driving force behind rheological characteristics, such as water binding and viscosity. Agoda-
94 Tandjawa (2012) reported that in the presence of calcium ions, low methoxyl pectin exhibited
95 a synergistic effect with MFC fibres leading to increased shear and complex viscosities of the
96 composites. In the present study, the impact of carboxymethyl cellulose on rheological
97 properties of a dried and redispersed MFC suspension was studied.

98 It has been suggested that proton nuclear magnetic resonance (NMR) parameters such as spin-
99 lattice-relaxation time (T_1) and spin-spin relaxation time (T_2) are sensitive to water state and
100 mobility in polymeric suspensions/dispersions (Ono, Inamoto and Okajima, 1997; Rachocki,
101 Markiewicz and Tritt, 2005, Vackier, Hills and Rutledge, 1999). The spin-spin relaxation time

102 T₂ is generally measured using the Carr-Purcell-Meiboom-Gill (CPMG) pulse sequence
103 (Meiboom and Gill, 1958). The CPMG sequence provides a more accurate measure of the
104 liquid transverse free-induction decay time (T₂) and is free of artefacts such as magnetic
105 inhomogeneity. In a study by Ono (1997), an MCC suspension was shown to contain both free-
106 water and water-associated to the polymer with a mutual exchange of protons resulting in
107 shorter overall T₂ compared to pure distilled water, where a typical T₂ is of the order of 2
108 seconds.

109 The primary aim of this study then is focused on understanding the impact of CMC on the
110 redispersibility of MFC in water and its impact on rheological properties of the suspension. It
111 is hoped that this understanding will shed light on the occurrence of aggregation of MFC and
112 the technical problems that ensue from this in various industries from food to paper-making. A
113 detailed study of rheological behaviour and the NMR determined apparent water mobility of
114 the redispersed MFC/CMC system, when correlated with fluorescence microscopy, as
115 presented here, will enable important structural features of these cellulosic materials which are
116 of relevance to the food and personal care industries to be determined. The hypothesis
117 underpinning this research is that the addition of CMC to an MFC suspension improves the
118 redispersibility of MFC after drying, by increasing the repulsion between polymer chains due
119 to the charge on the added polymer, and that the effects on the apparent water mobility in the
120 matrix are ultimately due to this.

121 **2. Materials and methods**

122 *2.1. Materials*

123 Microfibrillar cellulose (MFC) from spruce cellulose (8.97% w/w MFC paste) was provided by
124 Borregaard AS (Sarpsborg, Norway). Cellulose was obtained from 100% spruce. The charge
125 density of pure cellulose changes noticeably during the pre-treatment and finishing process to
126 produce MFC (Ribitsch *et al.*, 2001). From the information provided by the supplier, the charge

127 density on the microfibrillar cellulose will be low. Carboxymethyl cellulose (CMC) with a
 128 degree of substitution of 0.71 was supplied by CP Kelco (Norway). Reverse osmosis (RO)
 129 water was used for all experiments. Light mineral oil density 0.838 g/mL at 25°C (Sigma-
 130 Aldrich, UK) was used during the rheological measurements to prevent sample dehydration.

131 *2.2. Sample preparation and biopolymer mixtures*

132 2% w/w aqueous suspensions of microfibrillar cellulose were prepared by diluting the MFC
 133 stock solution (8.97%w/w MFC paste) with RO water using a high shear overhead mixer
 134 (Silverson, UK) at 8000rpm for 5minutes. An aqueous solution of CMC (2% w/w) was
 135 prepared separately and added to a 2%w/w MFC suspension according to the formulations
 136 shown in Table 1, to produce an overall concentration including both components of 2%. The
 137 CMC sample was dissolved by dispersing in RO water (2%w/w) under gentle stirring (IKA
 138 Eurostar 20 Digital Overhead Stirrer) at room temperature for 2h. The pH of the solution was
 139 adjusted to 6.8 and left overnight at 4°C before mixing with the MFC stock suspension. Sodium
 140 azide solution (0.02% w/w) was added to prevent bacterial contamination. The concentration
 141 of stock samples was determined by evaporating to dryness and measuring the dry solids
 142 content.

143 *Table 1: Composition of the MFC/CMC model systems used in this study.*

Sample Code	% w/w in suspension	
	MFC (%)	CMC (%)
MFC100	2	0
CMC15	1.7	0.3
CMC25	1.5	0.5
CMC50	1	1

144 MFC/CMC solutions were mixed in different proportions as shown in Table 1 at room
 145 temperature in water and at an overall concentration of 2% w/w. All samples were mixed
 146 thoroughly using an overhead stirrer (Silverson, UK) at 8000rpm for 5minutes. The mixtures
 147 were stored overnight at room temperature for equilibration and the pH was re-measured. For

148 re-dispersion studies, an approximately 1mm thin layer of the suspension was layered on an
149 aluminium plate and dried at 50°C for 12 hours using a conventional oven (Gallenkamp hotbox
150 oven, size 2).

151 For rheological and relaxation NMR measurements all dry samples were redispersed at 2% w/w
152 concentration in water by using high shear (T25 digital Ultra-Turrax®) at 15000rpm for
153 4minutes at room temperature. Samples were stored overnight at room temperature on a roller
154 bed (Stuart Digital tube rollers - SRT6D) at a speed 60rpm in order to achieve a homogeneous
155 suspension. For relaxation NMR v/s shear viscosity curves, MFC100 and CMC15 “never-dry”
156 (ND) and “dried” (D) suspensions at 0.2-2% w/w were prepared in RO-water using high shear
157 (T25 digital Ultra-Turrax®) at 15000rpm for 4minutes at room temperature. The pH of all
158 suspensions was maintained at 6.8.

159 2.3. *Rheological measurements*

160 The rheological measurements were carried out on a stress-controlled rheometer (Physica MCR
161 301, Anton Paar, Austria) with a serrated parallel plate geometry (50mm diameter with a gap
162 of 1mm) at 20±1°C, controlled by a Peltier system. Small oscillatory amplitude sweeps were
163 generated by log ramping strain 0.01 to 100% at a constant frequency of 1Hz. Frequency
164 sweeps were performed over the frequency range of 0.1-15Hz at a constant strain of 0.2%
165 which lay within the linear viscoelastic region. Shear viscosity was measured at constant shear
166 rate *i.e.* at 50s⁻¹ at 20±1°C. Temperature sweeps were generated by heating the sample between
167 the plates from 20°C to 90°C at the rate of 1°C/min. During these experiments, the strain was
168 fixed at 1% and the frequency at 1Hz. A light mineral oil barrier was used to prevent water
169 evaporation. Data presented are an average of four replicates.

170 2.4. *Pulsed ¹H-NMR measurements*

171 Time domain measurements were carried out at 25MHz using a Resonance Instruments (RI)
172 Maran benchtop NMR spectrometer (Oxford-Instruments Plc, UK). This type of instrument is
173 used routinely in the food industry for fat and moisture measurements. The temperature was
174 regulated at $20\pm 1^{\circ}\text{C}$ by a conventional gas flow system calibrated with an external
175 thermocouple and controlled with a standard R.I. temperature unit. All measurements were
176 made in 10mm outer diameter (OD) NMR tubes. Spin-spin relaxation times (T_2) were recorded
177 using the CPMG (Carr-Purcell-Meiboom-Gill) pulse sequence (Meiboom and Gill, 1958),
178 $90^{\circ}_x - (\tau - 180^{\circ}_y - \tau - \text{echo})_n$ with $\tau = 2048\mu\text{s}$. Typical 90° pulse lengths were of the order
179 of $5\mu\text{s}$ and 180° pulse length was $10\mu\text{s}$. The recycle delay time was fixed at 10 seconds ensuring
180 that all samples were relaxed before the next pulse sequence was applied. 64 scans were
181 recorded. All samples were left at a constant temperature for 15min to ensure the temperature
182 was equilibrated and consistent for all data points (see McConville, Pope, 2001). All relaxation
183 curves obtained by the CPMG method showed a single exponential decay.

184 2.5. Microscopic analysis

185 Light microscopy of aqueous suspensions of samples was performed using an Olympus BX5
186 bright field light microscope at 20X magnification with a scale bar of $200\mu\text{m}$. The fibres were
187 dyed using Congo red dye (Sigma-Aldrich). Fluorescence microscopy was carried out using an
188 EVOS microscopy system in fluorescence mode with a 20X objective. As both MFC and CMC
189 do not fluoresce, it was necessary to attach a fluorescence label to one of them. In the current
190 study, CMC was tagged with FITC fluorescent dye. 1g of CMC was dissolved in 10ml of
191 dimethyl sulphoxide containing a few drops of pyridine. 0.1g of Isothiocyanate -fluorescein
192 was added to 20mg dibutyltin dilaurate and the whole mixture was heated at 95°C for 2hours.
193 Free dye was removed from the system by a number of precipitations in ethanol, then the FITC-
194 CMC was filtered and dried at 80°C . The protocol used is the same as that published by Belder
195 *et al.*, 1973.

196 3. Results and Discussion

197 3.1. Viscoelastic properties of MFC/CMC suspensions

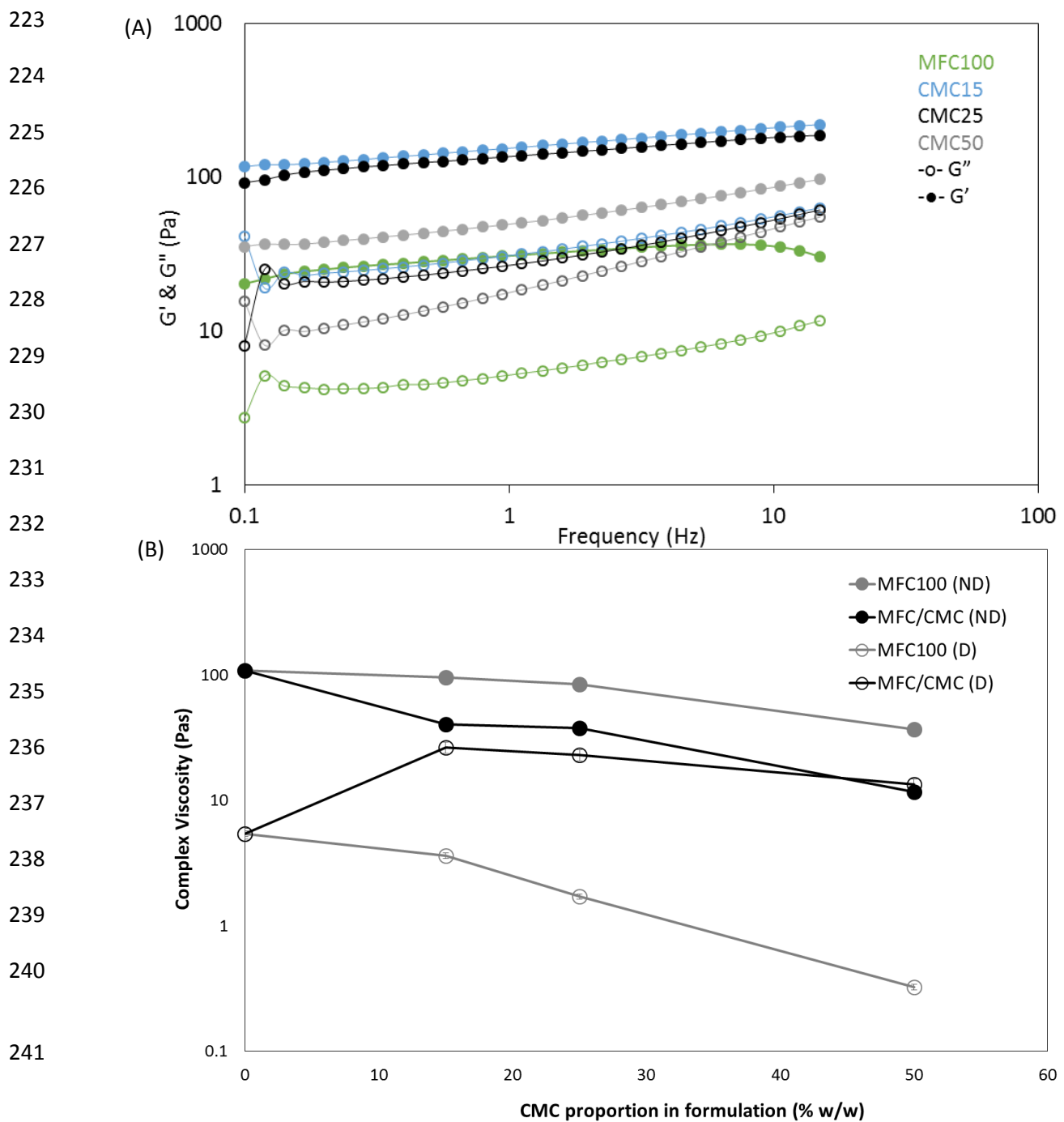
198 Figure 1A shows the viscoelastic properties as a function of frequency at 20°C for rehydrated
199 aqueous suspensions of MFC/CMC with various contents of CMC (CMC15, CMC25 and
200 CMC50), at a total biopolymer concentration of 2%w/w. The storage modulus (G') of the
201 suspension was higher than the loss modulus (G'') with little dependency on frequency
202 indicating viscoelastic gel-like behaviour. Both moduli increased with increasing frequency,
203 indicating that the network structure formed by the microfibrils is in the dynamic mode of
204 forming entanglements resulting in a stable network of fibres. Similar viscoelastic gel-like
205 behaviour was also observed with never-dried MFC100 and MFC/CMC suspensions.
206 Frequency sweep data for these systems are not shown. Similar viscoelastic behaviour was
207 observed with aqueous suspensions of softwood MFC containing polymeric additives such as
208 pectin, cationic starch *etc.* (Lowys, Desbrieres and Rinaudo, 2001; Tandjawa *et al.*, 2012).
209 Redispersed MFC/CMC suspensions showed noticeably higher values for G' and G'' compared
210 with MFC100 (Figure 1A). Visually, it was observed that the addition of CMC improved the
211 redispersibility of the MFC in water and a homogenous suspension was produced using a high
212 shear mixing process. Figure 1B shows the change in complex viscosity measured at 0.2%
213 strain and 1Hz frequency for pure MFC100 (D) without additives and MFC/CMC mixtures, as
214 a function of CMC proportion in the mixture. In Figure 1B, the concentration for pure MFC100
215 is identical to that present in MFC/CMC mixtures. It was observed that the complex viscosity
216 ($|\eta^*|$) of the redispersed suspension increased with an increase in CMC proportion in the
217 formulation, indicating that the MFC forms entangled networks crosslinked with CMC,
218 resulting in higher complex viscosity (Figure 1B) and higher values for G' and G'' (Figure 1A).

219

220

221

222

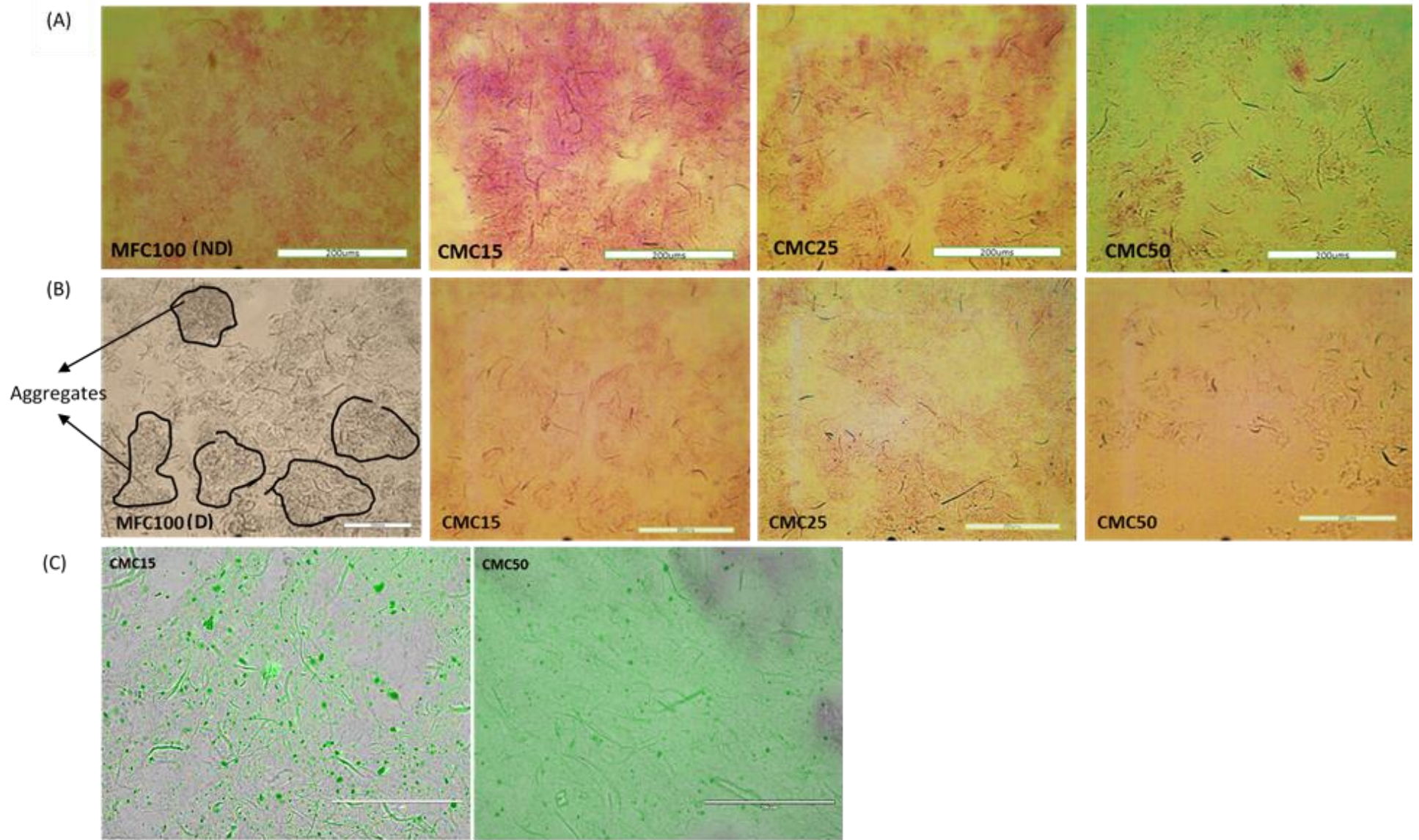


243 **Figure 1** (A) Frequency dependency of viscoelastic moduli for MFC/CMC mixtures dried and
 244 redispersed in aqueous media. Data were acquired at 0.2% strain and 20°C. Solid symbols
 245 represent the storage modulus (G') and open symbols the loss modulus (G''). (B) Complex
 246 viscosity η^* measured at a frequency of 1Hz and 0.2% strain as a function of CMC
 247 concentration in an aqueous suspension of MFC:CMC and also for MFC100 alone. For each
 248 point the MFC concentrations are matched therefore the percentage of MFC in a pure solution

249 *is identical to that present in an MFC/CMC formulation. At 0% CMC concentration the MFC*
250 *concentration is 2% and at a CMC concentration of 50% the MFC concentration is 1%. Solid*
251 *symbols represent the (ND) suspensions and open symbols the (D) suspensions.*

252 A noticeable difference in complex viscosity was observed on comparing the MFC100 (ND)
253 and MFC/CMC (ND) suspension (Figure 1B), this behaviour can be explained by the dilution
254 effect of CMC on MFC producing the different ratios. Diluting the MFC network structure
255 with CMC to make up the formulation (as per Table 1), results in less microfibril entanglement
256 in the network structure and is also seen in the microscopy images presented in Figure 2A,
257 resulting in a lower complex viscosity as compared with comparable concentrations of
258 MFC100 (ND) (Figure 1B). A slightly lower complex viscosity was observed when comparing
259 MFC/CMC (ND) and MFC/CMC (D) formulations, but this reduction was minimal in the case
260 of CMC50 (Figure 1B). However, the CMC50 suspension showed weaker gel-like behaviour.
261 The slight frequency dependence of the moduli and the relatively large value of $\tan \delta$ ($G''/G' > 0.1$)
262 defines so-called weak gel behaviour (Ikeda and Nishinari, 2001) as evident in Figure
263 1A. $\tan \delta$ values are also presented later in Figure 4. When the negatively charged CMC was
264 added at higher levels, the CMC adsorption to MFC increased significantly. Similar behaviour
265 was reported with bacterial cellulose/CMC systems where changes in zeta-potential were
266 shown (Veen *et al.*, 2014). The increase in the charge for all ratios of CMC leads to better
267 redispersibility of the MFC/CMC formulations in water with higher complex viscosity values.
268 Lower values of G' where $\tan \delta > 0.1$ for CMC50 suspensions can be explained by a dilution
269 effect. As the dense network of microfibrils plays an important role in maintaining viscoelastic
270 gel-like behaviour, when MFC is diluted with 50% CMC the MFC is at 1%, which without
271 additives shows an order of magnitude decrease in G' and G'' (Figure 1B), and the MFC forms
272 a weaker entangled network structure.

273
274
275
276
277
278
279
280
281
282
283
284
285
286
287
288



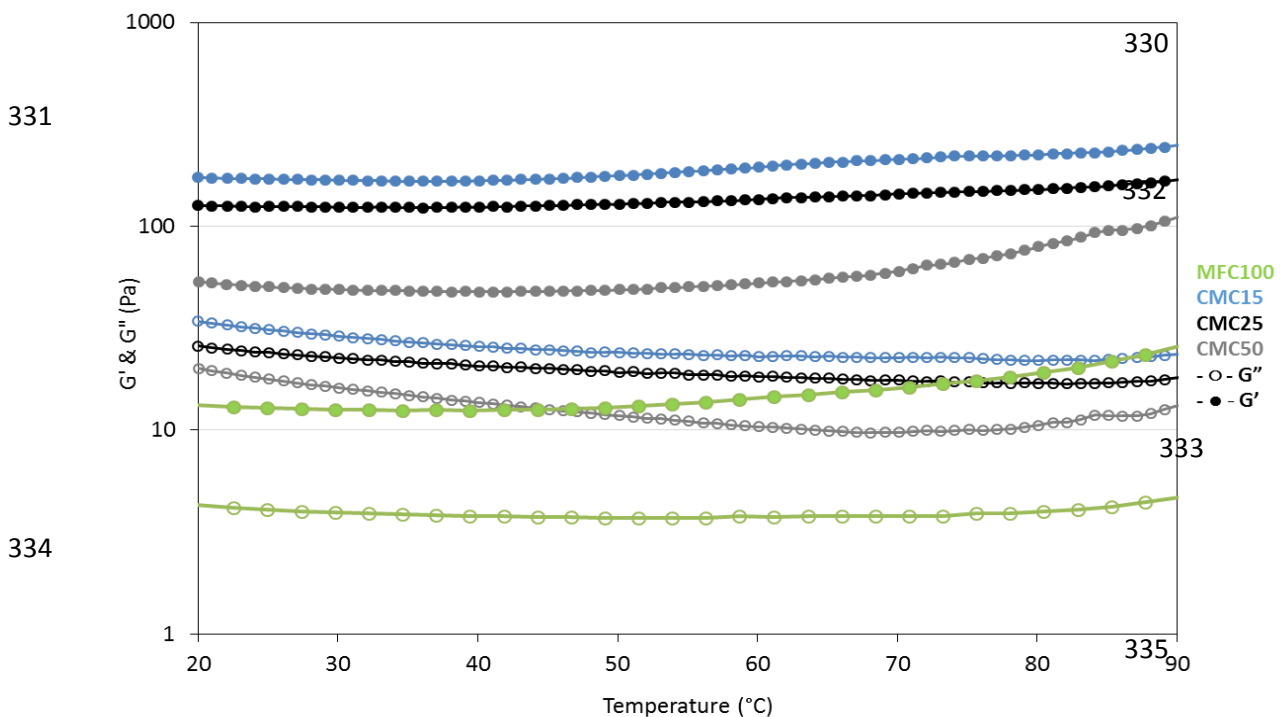
289 **Figure 2** *Light microscopy images of 2% w/w aqueous suspensions of (A) never dried, (B)*
290 *dried and redispersed suspensions of MFC100 and MFC/CMC at CMC levels of 15, 25 and*
291 *50%. (C) Fluorescence microscopy images of 2% w/w redispersed suspension of CMC15, and*
292 *CMC50, scale bar 200 μ m, where CMC is tagged with FITC (green fluorescence).*

293 Light microscopy images of never-dried MFC with different levels of CMC indicated that the
294 addition of CMC does not affect microfibrillar entangled network except at high levels (Figure
295 2A). A lower level of entanglement was observed in the case of CMC50. This can be explained
296 by dilution effect of CMC on the MFC network structure as outlined for the case of complex
297 viscosity earlier. Microscopy images of dried and redispersed MFC/CMC (i.e., CMC15,
298 CMC25 & CMC50) indicate that the addition of CMC reduced the microfibrillar aggregate or
299 fibre bundle formation as compared to MFC100 (D) (Figure 2B). Drying MFC without CMC
300 resulted in a large amount of microfibrillar aggregates due to the formation of strong inter- and
301 intramolecular hydrogen bonds during the drying process (Figure 2B). These were difficult to
302 redisperse in water and reduced the values of viscoelastic parameters such as G' , G'' and
303 complex viscosities due to poor network formation. From fluorescence microscopy images
304 (Figure 2C) it cannot be said with certainty that fluorescently tagged-CMC interacted at a
305 molecular level with the surface of MFC microfibrils. It is strongly implied however from the
306 comparison in Figure 2C of CMC15 and CMC50 that as the amount of CMC increased, either
307 the surface coverage of MFC by CMC increased or there was a general build-up of the labelled
308 CMC in the solution surrounding the fibres.

309 *3.2. Temperature dependence of the viscoelastic moduli*

310 The temperature dependence of G' and G'' for 2% w/w aqueous suspensions of MFC/CMC
311 mixtures is shown in Figure 3. All the samples showed stable viscoelastic gel-like behaviour
312 where the storage modulus was higher than the loss modulus throughout the temperature range
313 20°C - 90°C at a heating rate of 1°C/min. It was observed that the G' and G'' for all suspensions

314 showed an initial slight decrease from 20°C to 40°C, however above 40°C the suspensions
 315 showed an increase in G' and G'' up to 90°C. Similar behaviour was observed with cellulose
 316 nanofibers from poplar wood by Chen *et al.*, 2013. The first slight decrease in modulus may be
 317 due to thermal agitation/thermal motion of microfibrils, resulting in loosening of the fibrils
 318 within the network structure. However, the swelling of microfibrils with an increase in
 319 temperature, while interacting with CMC in the matrix, may strengthen the gel-like structure,
 320 resulting in an increased G' and G'' of suspensions above 40°C. As the amount of CMC
 321 increased in the formulation, G' and G'' increase to a greater extent above 40°C suggesting
 322 synergistic interactions between MFC/CMC. It is well known that polymeric solutions such as
 323 HPMC (hydroxyl propyl methyl cellulose), exhibit an increased thermal motion upon heating,
 324 leading to a weaker network and sometimes a decrease in viscosity, however the viscosity of
 325 these systems tends to increase above the gelation temperature depending on concentration
 326 (Silva *et al.*, 2008). The fact that the MFC/CMC suspensions do not lose structure upon heating,
 327 even when the MFC proportion is lowered, indicates an interaction beyond the surface
 328 stabilisation of the microfibrils by CMC, although it is not yet clear which mechanisms are
 329 involved.



336 **Figure 3** *Temperature dependency (20° to 90°C at a heating rate 1°C/min) of the viscoelastic*
337 *moduli of 2% w/w aqueous suspensions of MFC100 (D) and MFC/CMC (D) acquired at 1Hz*
338 *frequency and 1% strain. Solid symbols represent storage modulus (G') and open symbols*
339 *represent loss modulus (G'').*

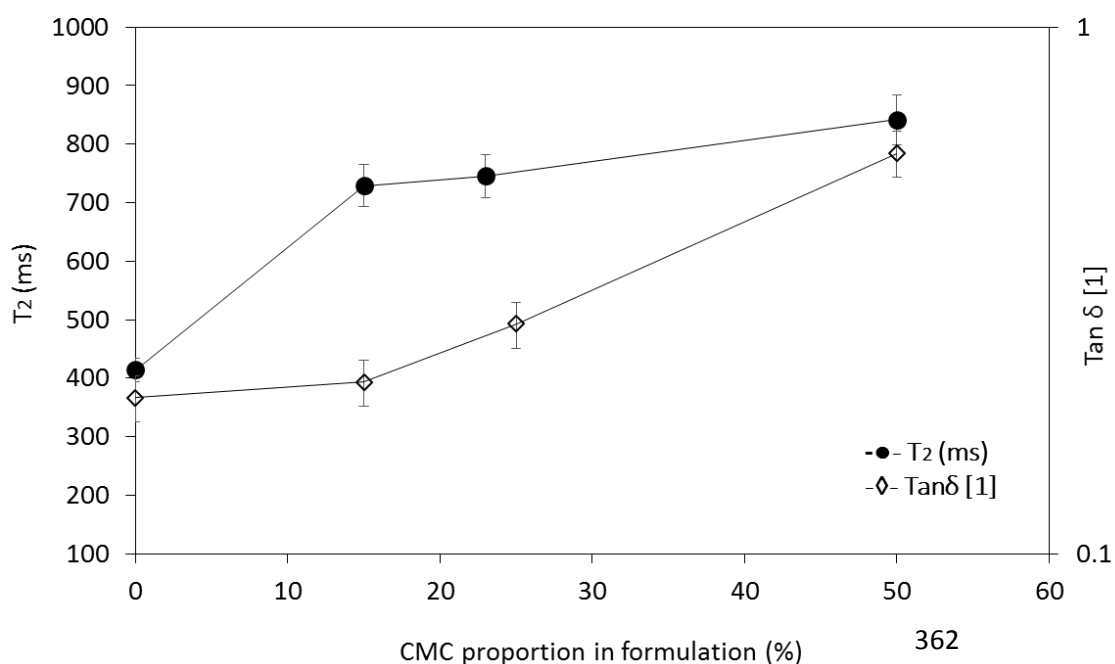
340 3.3. Relaxation time (T_2) of MFC/CMC suspensions

341 Figure 4 shows the spin-spin relaxation time (T_2) as a function of the amount of CMC present
342 in the MFC/CMC formulations. At higher levels of CMC in the formulation, the T_2 (ms) value
343 and the $\tan \delta$ of the suspension increased, the latter implying that the suspension was behaving
344 in a more viscous or liquid-like fashion. Lower T_2 values for the redispersed MFC100
345 (CMC=0) suspensions are most likely due to the rigid network structure formed by strong intra-
346 or intermolecular H-bond within the microfibrils and a consequently reduced T_2 value for the
347 polymeric component. It appears to be the presence of these rigid structures in case the of
348 MFC100 (D) suspensions which dominate the T_2 values at all concentrations. In this case, the
349 overall T_2 value of the suspensions are driven by the T_2 value of the polymer “ $1/T_{2p}$ ” (see
350 equation 1) assuming the water is behaving as bulk water and has not been perturbed in any
351 way. The fraction of water which is proposed to be perturbed in such systems is normally low
352 (~2%, McConnell & Pope 2001).

$$353 \quad 1/T_2 = a*(1/T_{2p}) + (1-a)*(1/T_{2w}) \quad \text{Equation (1)}$$

354 Equations of the form of equation 1 describe the effect of protons exchanging between a
355 polymer site with the polymer present at a weight fraction a and having a T_2 value of T_{2p} and
356 water at a weight fraction $(1-a)$ having a T_2 value of T_{2w} under conditions of a CPMG Tau
357 value which allows exchange to be rapid. To examine the effect of drying on the overall
358 apparent water mobility in the microfibrillar network in the presence and absence of CMC, the
359 T_2 values and shear viscosities as a function of concentration were plotted for aqueous

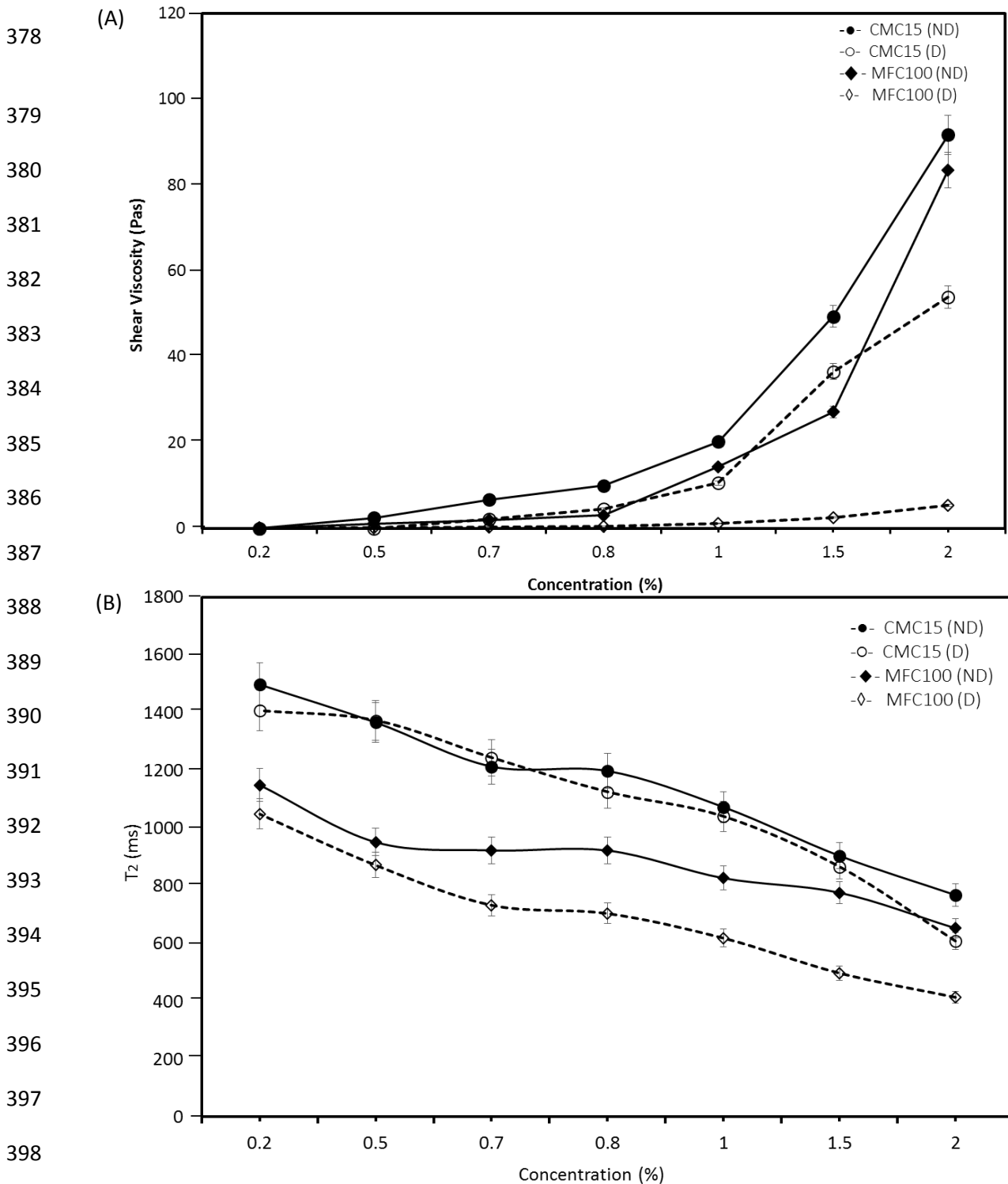
360 suspensions of CMC15 (ND) which had not been dried, CMC15 (D) which had been dried but
 361 then redispersed and compared with MFC100 (ND) and MFC100 (D) (Figure 5A and 5B).



363 **Figure 4** Change in T_2 (ms) and $\text{Tan}\delta$ (measured at a frequency of 1 Hz and a strain of 0.2%)
 364 plotted against increasing proportion of CMC in the suspension at 20°C.

365 As suggested earlier, the drying of MFC without CMC results in the formation of strong
 366 intermolecular H-bonds between the microfibrils resulting in rigid fibre bundles or aggregates
 367 of MFC, which limits the polymer mobility within the microfibril network resulting in lower
 368 redispersibility. Effectively this reduces the T_{2p} value of the polymer and consequently
 369 increases the $1/T_{2p}$ value reducing the overall measured T_2 as can be seen in figure 5B. As the
 370 concentration increases, this effect becomes more pronounced however now it is mediated by
 371 increases in the value of a . The net result is a further decrease in the value of T_2 . If the polymer
 372 is not dried then the bonding between the fibrillar complex is not as strong and the T_2 values
 373 are higher by similar arguments to the above. Figure 5A shows that the addition of CMC to
 374 MFC *i.e.* CMC15 (D) significantly increases the shear viscosity of the redispersed suspension
 375 compared to MFC100 (D). Similarly, the overall T_2 values of the redispersed CMC15 (D) were

376 higher compared to MFC100(D) (Figure 5B). The CMC15(ND) suspensions showed highest
 377 T_2 values of all.



399 **Figure 5** (A) Shear viscosity (at $50s^{-1}$ shear rate); and (B) Spin-spin relaxation time T_2 (ms) as
 400 a function of concentration at $20^{\circ}C$ for (-◇-) MFC100 (ND) solid diamonds, (D) unfilled
 401 diamonds; (-○-) CMC15 (ND) solid circles, (D) unfilled circles.

402 The addition of CMC appears to prevent the formation of strong hydrogen bonds between MFC
403 fibres, resulting in improved redispersibility of the CMC15. The reduced amount of aggregates
404 and fibres bundles in the redispersed suspension increases polymer mobility and hence
405 increases the polymer T_2 value in the CMC15. There may also be a direct effect of the CMC
406 on the polymer via an altered ionic environment. The result of these changes is that the
407 interactions between fibrils are weaker and the overall measured T_2 increases. If this
408 interpretation is correct then whilst the NMR T_2 value is sometimes loosely referred to as the
409 water signal it is in fact actually only the apparent overall water mobility. Equation 1 gives a
410 more accurate description of mobility in the system. In addition, because the bonds are now
411 weakened by CMC, the difference in T_2 values between the dried and non-dried CMC
412 containing materials is reduced as can be seen in Figure 5B. Drying the MFC100 systems
413 results in tighter bonding which impairs redispersibility and results in substantial differences
414 between dried and non-dried MFC100.

415 **4. Conclusions**

416 The influence of CMC on the rheological properties of MFC suspension is consistent with an
417 exchange based NMR interpretation of spin-spin relaxation times (T_2) for polymer and water.
418 Rheological measurements show that addition of CMC to MFC increases complex viscosity
419 and shear viscosity of the suspension compared to dried MFC without additives. Fluorescence
420 microscopy showed that the CMC tends to interact homogeneously with MFC possibly on the
421 surface of the microfibrils present in the network. This prevents the formation of H-bonds
422 between the MFC's microfibrils, hence making dried MFC/CMC easier to redisperse in water.
423 The lower T_2 -values of the single component MFC100 suspensions result from the rigid
424 structures formed upon drying and the lower polymer mobility. The addition of CMC to the
425 MFC suspensions improved redispersibility of MFC after drying and produces stable and

426 highly fibrillated microstructures, hence increasing apparent water mobility (T_2 values) within
427 the matrix.

428 **Acknowledgement**

429 This work was supported by the Oslofjordfond, Norway grant scholarship (2012 - 2015).

430 **References**

431 Agoda-Tandjawa G., Durand S., Berot S., Blassel C., Gaillard C., Garnier C., Doublier L.J.
432 (2010) Rheological characterization of microfibrillated cellulose suspensions after freezing.
433 Carbohydrate Polymers 80, 677-686.

434 Agoda-Tandjawa G., Durand S., Gaillard C., Garnier C., Doublier J.L., (2012) Rheological
435 behaviour and microstructure of microfibrillated cellulose suspensions/low-methoxyl pectin
436 mixed systems. Effect of calcium ions. Carbohydrate Polymers. 87-2, 1045–1057.

437 Andresen M., Stenstad P., Møretrø T., Langsrud S., Syverud K., Johansson L.S., Stenius P.
438 (2007). Nonleaching Antimicrobial Films Prepared from Surface-Modified Microfibrillated
439 Cellulose. Biomacromolecules. 8-7, 2149–2155

440 Belder De. N.A, Granath K. (1973) Preparation and properties of fluorescein-labelled dextrans.
441 Carbohydrates Research. 30, 375-378.

442 Bruce D.M., Hobson R.N., Farrent J.W., Hepworth D.G. (2005). High-performance composites
443 from low-cost plant primary cell walls. Composites Part A: Applied science and
444 Manufacturing. 36-11, 1486–1493.

445 Burger C., Hsiao B.S., Chu B. (2006). Nanofibrous Materials and Their Applications. Annu
446 Rev Mater Res. 36, 333–368.

447 Chen P., Yu H., Liu Y., Chen W., Wang X., Ouyang M. (2013) Concentration effects on the
448 isolation and dynamic rheological behaviour of cellulose nanofibers via ultrasonic processing.
449 Cellulose. 20,149-157.

450 Cordoba A., Camacho M.D.M., Navarrete N.M. (2010). Rheological behaviour of an insoluble
451 lemon fibre as affected by stirring, temperature, time and storage. Food and Bioprocess
452 Technology. 5-3, 1083-1092.

453 Fernandes D.J.M.B., Gil M.H., Castro J.A.A.M. (2004). Hornification-its origin and
454 interpretation in wood pulps. *Wood Science and Technology*. 37, 489-494.

455 Frone, A. N., Panaitescu, D. M., & Donescu, D. (2011). Some aspects concerning the isolation
456 of cellulose micro- and nano-fibers. *U.P.B. Science Bulletin, Series B*. 73-2, 133–152.

457 Henriksson M., Henriksson, G., Berglund, L. A., & Lindstrom, T. (2007) An environmentally
458 friendly method for enzyme-assisted preparation of microfibrillated cellulose (MFC)
459 nanofibers. *European Polymer Journal*, 43, 3434–3441.

460 Herrick F.W., Casebier R.L., Hamilton J.K., Sandberg K.R. (1983). Microfibrillated cellulose:
461 morphology and accessibility. *J Appl Polym Sci: Appl Polym Symp*. 37-9,797–813.

462 Ikeda S., Nishinari K. (2001). “Weak Gel”-Type Rheological Properties of Aqueous
463 Dispersions of Non-aggregated K-Carrageenan Helices. *Journal of Agriculture Food*
464 *Chemistry*. 49, 4436–4441.

465 Kato K.L., Cameron R.E., (1999). A review of the relationship between thermally-accelerated
466 ageing of paper and hornification. *Cellulose*. 6, 23-40.

467 Khopade A.J., Jain N.K. (1990). A Stable Multiple Emulsion System Bearing Isoniazid:
468 Preparation and Characterization. *Drug Dev Ind Pharm*. 24-3, 289–293.

469 Kirk R.E., Othmer D.F. *Cellulose, Encyclopedia of chemical technology* (2nd ed.) Wiley, New
470 York. 4

471 Kocherbitov V., Ulvenlund S., Kober M., Jarring K., Arnebrant T. (2008) Hydration of
472 microcrystalline cellulose and milled cellulose studied by sorption calorimetry. *J.*
473 *Phys.Chem.B*. 112. 3728-3734.

474 Lavoine N., Desloges I., Dufresne A., Bras J. (2012). Microfibrillated cellulose – Its barrier
475 properties and applications in cellulosic materials: A review. *Carbohydrate Polymers*. 90-2,
476 735–764.

477 López-Rubio A, Lagaron J.M., Ankerfors M., Lindström T., Nordqvist D., Mattozzi A.,
478 Hedenqvist M.S. (2007). Enhanced film forming and film properties of amylopectin using
479 micro-fibrillated cellulose. *Carbohydrate Polymers*. 68-4,718–727.

480 Lowys M.P., Desbrières, J., Rinaudo, M. (2001) Rheological characterization of cellulosic
481 microfibril suspensions: Role of polymeric additives. *Food Hydrocolloids*. 15,25-32.

482 Malainine M.E., Mahrouz M., Dufresne A. (2005). Thermoplastic nanocomposites based on
483 cellulose microfibrils from *Opuntia ficus-indica* parenchyma cell. *Composites Science*
484 *Technology*. 65-10, 1520–1526.

485 McConville P, Pope J.M. (2001). ¹H NMR T₂ relaxation in contact lens hydrogels as a probe
486 of water mobility. *Polymer*. 42(8), 3559–3568.

487 Meiboom S. and Gill, D (1958) Modified spin-echo method for measuring nuclear relaxation
488 times. *Rev. Sci. Instrum.* 29, 688-691.

489 Missoum K., Bras J., Belgacem N.M., (2012). Water redispersible dried nanofibrillated
490 cellulose by adding sodium chloride. *Biomacromolecules*. 13, 4118-4125.

491 Nakagaito A.N, Yano H. (2004). The effect of morphological changes from pulp fiber towards
492 nano-scale fibrillated cellulose on the mechanical properties of high-strength plant fiber based
493 composites. *Appl Phys A: Mater Sci Process*. 78-4, 547–552.

494 Nishiyama Y., (2009) Structure and properties of the cellulose microfibril. *J Wood Sci*. 55,241-
495 249.

496 Norton I.T., Foster, T.J., Brown, R. (1998). The science and technology of fluid gels. *Gums*
497 *and stabilisers for the food industry*. Ed. William, P.A., Phillips, G.O. Edition 9; 259-268.

498 Ono H., Inamoto M., Okajima K., (1997) Spin-lattice relaxation behaviour of water in cellulose
499 materials in relation to the tablet forming ability of microcrystalline cellulose particles.
500 *Cellulose*. 4, 57–73.

501 Ougiya H., Watanabe K., Morinaga Y., Yoshinaga F. (1997). Emulsion-stabilizing Effect of
502 Bacterial Cellulose. *Biosci Biotechnol Biochem*. 61-9, 1541–1545.

503 Oza K.P., Frank S.G.J.J. (1986). Microcrystalline Cellulose Stabilized emulsions. *Dispersion*
504 *Sci Technol*. 7-5, 543–561.

505 Pääkkö M., Ankerfors M., Kosonen H., Nykänen A., Ahola S., Österberg M., Ruokolainen J.,
506 Laine J., Larsson P.T., Ikkala O., and Lindström T. (2007). Enzymatic Hydrolysis Combined
507 with Mechanical Shearing and High-Pressure Homogenization for Nano-scale Cellulose Fibrils
508 and Strong Gels. *Biomacromolecules*. 8, 1934-1941.

509 Quievy N., Jacquet N., Sclavons M., Deroanne C., Paquot M., Devaux J. (2010) Influence of
510 homogenization and drying on the thermal stability of microfibrillated cellulose. *Polymer*
511 *degradation and stability*. 95,306-314.

512 Rachocki A., Markiewicz E., Goc-Tritt J. (2005) Dielectric relaxation in cellulose and its
513 derivatives. *Acta Physica Polonica A*. 108, 137-145.

514 Ribitsch V., Stana-Kleinschek K., Kreze T., and Strnad S. (2001). The significance of surface
515 charge and structure on the accessibility of cellulose fibres. *Macromolecular Materials and*
516 *Engineering*. 286, 648-654.

517 Silva S.M.C., Pinto, F.V., Antunes, F.E., Miguel, M.G., Sousa, J.J.S., Pais, A.A.C.C. (2008).
518 Aggregation and gelation in hydropropylmethyl cellulose aqueous solutions. *Journal of Colloid*
519 *and Interface Science*. 327, 333-340.

520 Smook G.A. (1990) Hornification (keyword). In: *Handbook of pulp & paper terminology*.
521 Angus Wilde, Vancouver, p 135.

522 Syverud K., Stenius P. (2009). Strength and barrier properties of MFC films. *Cellulose* 16, 75–
523 85.

524 Tatsumi D., Ishioka S., & Matsumoto T. (2002). Effect of fibre concentration and axial ratio
525 on the rheological properties of cellulose fibre suspensions. *Journal of the Society of Rheology*
526 *Japan*. 30-1, 27–32.

527 Tatsumi, D. (2007). Rheology of cellulose fibre disperse systems and cellulose solutions.
528 *Nihon Reoroji Gakkaishi*. 35-5, 251–256.

529 Turbak A.F., Snyder F.W., Sandberg K.R. (1983). Microfibrillated cellulose, a new cellulose
530 product: properties, uses, and commercial potential. *J Appl Polym Sci: Appl Polym Symp*. 37,
531 815.

532 Vackier C.M., Hills B.P., Rutledge D.N. (1999) An NMR Relaxation study of the state of water
533 in gelatin gels. *Journal of Magnetic Resonance*. 138, 36–42.

534 Veen S.J., Kuijk, A., Versluis, P., Husken, H., Krassimir, P.V. (2014). Phase transitions in
535 cellulose microfibril dispersions by high-energy mechanical de-agglomeration. *Langmuir*. 30,
536 13362-13368.